Carbon nanotubes as fillers for composites with enhanced thermal conductivity

Andreas Klemenz,[1] Leonhard Mayrhofer,[1] Blanka Lenczowski,[2] and Michael Moseler[1,3,*]

[1]*Fraunhofer IWM, MicroTribology Centre μTC, Wöhlerstraße 11, 79108 Freiburg, Germany*

[2]*Airbus Defence and Space GmbH, Willy-Messerschmitt-Straße 1, 82024 Taufkirchen, Germany*

[3]*Institute of Physics, University of Freiburg, Hermann-Herder-Straße 3, 79104 Freiburg, Germany*

(Received 28 June 2021; accepted 26 July 2021; published 16 August 2021)

Thermal conductivities of single- and double-wall carbon nanotubes in contact with foreign atoms on their surfaces are investigated by means of molecular dynamics simulations. Small amounts of atoms on the surfaces of single-wall nanotubes drastically reduce their thermal conductivity, while the conductivities of the inner walls of double-wall nanotubes which are only weakly coupled to the outer walls are retained even for large amounts of atoms on the surfaces. Based on the simulation results, an estimation for the conditions under which an enhancement of thermal conductivities can be expected is presented.

DOI: 10.1103/PhysRevMaterials.5.086001

I. INTRODUCTION

Carbon-based nanostructures such as carbon nanotubes (CNTs) or graphene are materials with outstanding electronic, thermal, and mechanical properties [1]. While potential applications often focus on nanoelectronics and other nanotechnologies, composites of carbon nanostructures with metallic, organic, or ceramic matrices could also benefit from the exceptional properties of CNTs and graphene. Some areas of industrial relevance for such composites are mechanical reinforcement [1,2] or electromagnetic shielding and lightning protection of aircrafts [3]. Of special interest in the context of this article are thermal interface materials for enhanced heat dissipation in electronic devices. In recent decades, the number of transistors in microprocessors has roughly followed Moore's Law, doubling every 18 months. With the accompanying reduction in structure sizes, power densities increased dramatically and the amount of heat produced became increasingly problematic. As a result, large surface area metallic heat sinks must be placed on microprocessors to increase the amount of heat that can be dissipated by convection and thermal radiation. With further reductions in structure sizes in the future, cooling will become even more challenging than it is today. This has led to increasing interest in nonconventional materials such as diamond, graphene, and CNTs, which have much higher thermal conductivities than conventional heat sink materials and could therefore dissipate heat more effectively [4,5]. Due to the relatively low mass density of graphene and CNTs, composites thereof additionally fulfill the important requirement of weight reduction in space applications, where heat dissipation demands are becoming a major issue due to miniaturization of satellites or in future high-capacity telecommunication satellites. Experimental studies typically report thermal conductivities of roughly 3500 W/(m K) for single-wall nanotubes (SWNTs) with lengths of 2.5 μm [6]. This is about one order of magnitude higher than the thermal conductivities of aluminum [237 W/(m K)] and copper [401 W/(m K)] [7], which are usually used to build heat sinks. However, CNTs are difficult to handle and potentially pose a risk to human health. Direct coating of surfaces with CNTs is therefore critical, although there have been efforts in this direction [8,9]. Enclosing CNTs in a composite material would circumvent these problems and would therefore be suitable for technical applications.

Producing composite materials requires good distribution and dissipation of the filler in the matrix. In the case of CNTs, this is much easier to achieve with organic matrices than with metals. For this reason, many authors have studied the influence of CNTs on the thermal conductivity of organic materials (e.g., [10–14]), while there are few reports on metal matrix composites [1,4,15,16]. Experimental investigations of thermal conductivities of composites with organic matrices reach very different results without a clear trend. Some authors find a decrease, while others find an increase up to a factor of 5 [10]. Such an increase is interesting by itself, but since the absolute thermal conductivities of the resulting composites are still very low compared to metals, they are not suited for technical applications. Yu *et al.*, for example, report a conductivity of about 1 W/(m K) [10], which is two orders of magnitude lower than the conductivities of aluminum and copper. However, there is still some discrepancy between the results of experimental studies and theoretical estimations predicting much higher thermal conductivities for composites with CNTs. Huxtable *et al.* [17], for example, present a simple geometrical estimation for the expected thermal conductivity of the composite and find that the actual values are considerably lower. They attribute this discrepancy to the thermal resistance of the CNT-matrix contact and to phonon scattering caused by the interaction between the CNT wall and the matrix. Padgett and Brenner also find the latter in molecular dynamics simulations of CNTs with organic groups coupled to the CNT walls [18]. Moisala *et al.* studied single- and multiwall CNTs as fillers for polymer composites and found

*michael.moseler@iwm.fraunhofer.de

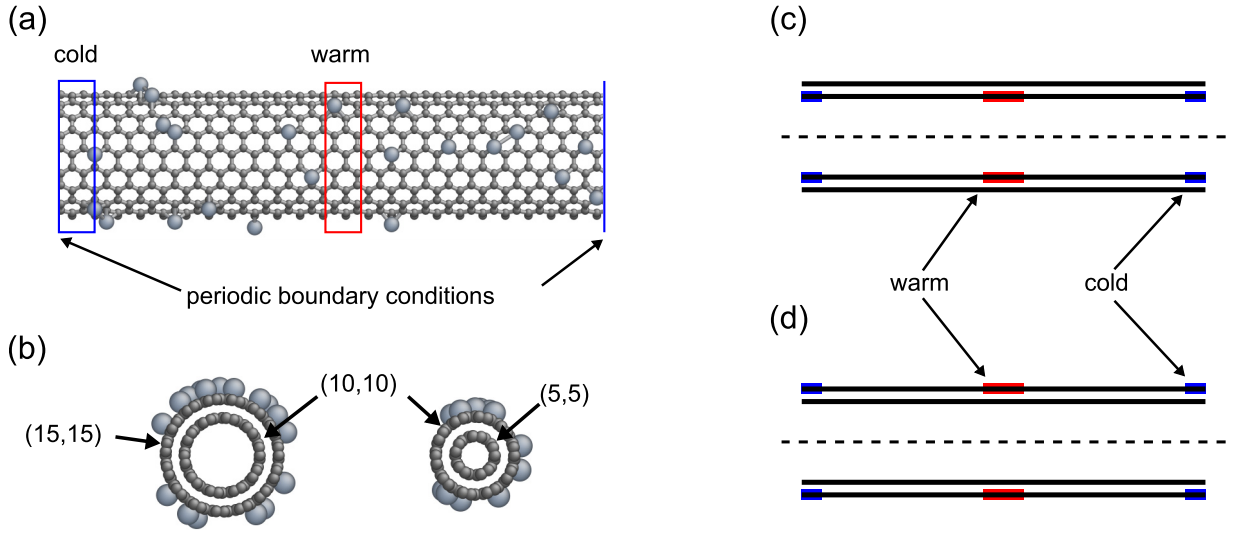

FIG. 1. (a) Simulation setup schematically shown for a (10,10) SWNT with 5% iron atoms on the surface. Slices at the edge and the center are coupled to heat baths with different temperatures to apply a temperature gradient along the CNT axis. (b) Cross sections through the investigated DWNTs. Iron atoms are attached to the outer walls only. Thermalization scheme for (c) (10,10)-(15,15) and (d) (5,5)-(10,10) DWNTs.

a decrease in thermal conductivity for single-wall CNTs and an increase for multiwall CNTs [19]. They also speculate that CNT-matrix interactions cause phonon scattering in SWNTs, reducing their thermal conductivity, while phonons can be transported through the inner walls without being affected by the matrix. However, they do not investigate this effect further. Boroushak *et al.* have performed molecular dynamics simulations of the thermal conductivities of single- and double-wall carbon nanotubes (DWNTs) functionalized with polyethylene chains. They report that the decrease in thermal conductivity due to the attached molecules is less pronounced in double-wall CNTs [20]. However, they also did not perform a deeper analysis of this effect.

In this work, we investigate thermal transport in single- and double-wall nanotubes by means of classical molecular dynamics simulations. We explicitly compare single- and double-wall CNTs and investigate the influence of the contact between the outermost CNT walls and foreign atoms to model interactions between CNTs and the matrix of a composite. Furthermore, we present an analytical model that provides deeper insight into the differences and allows us to estimate in which regime enhancements in the thermal conductivities of composites can be expected.

II. COMPUTATIONAL MODEL

We use classical molecular dynamics to investigate single- and double-wall CNTs in contact with iron atoms. The interatomic forces are modeled with a Tersoff-Brenner bond order potential [21,22] with parameters from Henriksson and Nordlund [23]. This parametrization provides an accurate description of the interactions between iron and carbon atoms, which is why we use iron instead of the typical heat sink materials aluminum and copper, for which such a parametrization is not available. In the case of DWNTs, we use an additional Lennard-Jones potential with parameters from Girifalco *et al.* [24] to model the interactions between CNT walls. This potential was originally developed for modeling buckyballs inside of CNTs and was later successfully applied to simulate the interactions between the walls of multiwall nanotubes (MWNTs) [25].

We investigate (10,10) SWNTs, and (5,5)-(10,10) and (10,10)-(15,15) DWNTs with different lengths in periodic supercells. Different amounts of iron atoms ranging from 0 to 20% are attached to the outer walls of the CNTs at random positions (Fig. 1). The percentage value indicates the ratio between the number of iron and carbon atoms in the case of SWNTs and the ratio between the number of iron atoms and the number of carbon atoms in the outermost wall in the case of DWNTs. After attaching the iron atoms to the surfaces, the systems are carefully relaxed to avoid disturbances of the conductivity measurements due to released energy during adatom rearrangements.

To measure the thermal conductivity of a system, one slice at the edge of the supercell is coupled to a Langevin thermostat at 290 K and one slice at the center is coupled to a thermostat at 310 K, each with a time constant of 0.01 ps [Fig. 1(a)]. The heat flux through the system is determined by recording the amounts of energy exchanged by the thermostats with the system during a time of at least 1 ns. Temperature profiles along the CNT axes are determined by dividing the systems into 3.5-nm-thick slices and averaging their temperatures over a period of at least 500 ps.

In most studies dealing with heat conduction, the three-dimensional (3D) thermal conductivity λ is reported, where λ is the proportionality constant between a temperature gradient ∇T and the resulting heat flux $\mathbf{j} = \dot{Q} A^{-1} \hat{\mathbf{n}}_A$ in the system: $\mathbf{j} = -\lambda \nabla T$. We want to point out that these definitions are not suitable for low-dimensional systems such as carbon nanotubes since their cross-sectional area is not a well-defined quantity. Many authors try to circumvent this problem by considering a ring around the CNT wall with a thickness of the distance between graphene layers in graphite as the cross-sectional area of a SWNT. This procedure is arbitrary

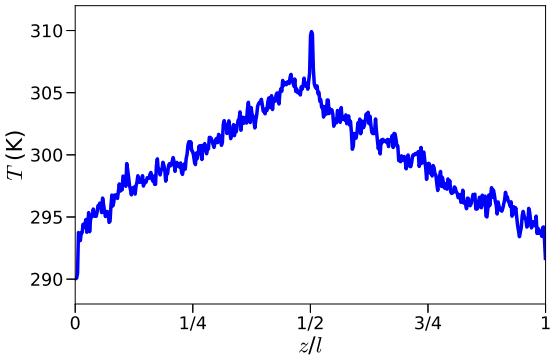

FIG. 2. Temperature profile in a 177-nm-long (10,10) SWNT with bare surface.

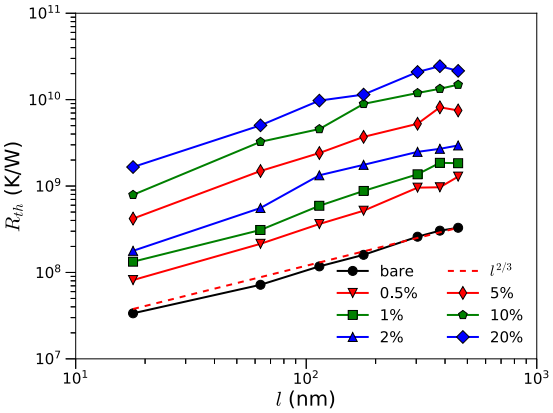

FIG. 3. Thermal resistances of bare SWNTs compared to SWNTs with different amounts of iron atoms coupled to the surface. The dashed line shows a χ^2 fit of a $l^{2/3}$ behavior to the data (see text for details).

and cannot be reasonably applied to multiwall nanotubes. Moreover, comparisons between SWNTs and DWNTs are not possible when these definitions are used. We therefore either report thermal resistances that are completely independent of cross-sectional area or, if it is more convenient to use conductivities, we use 2D conductivities and heat fluxes calculated with circumferences instead of cross-sectional areas. 3D conductivities are used only for comparing with other authors' results or for calculating bulk properties. In cases where the reader might get confused, we explicitly state where 2D and where 3D quantities are used.

III. RESULTS AND DISCUSSION

A. (10,10) SWNTs

As a first step, we investigate the influence of iron atoms on the thermal conductivity of (10,10) SWNTs. Typical temperature profiles in SWNTs are linear in the regions not coupled to thermostats and with distinct peaks in the thermostated regions (Fig. 2). These peaks become smaller as the amount of iron on the surfaces is increased. While the formation of a linear region between the thermostats can be easily explained by solving the heat equation in 1D without heat sinks and sources (see Sec. I in the Supplemental Material [26]), there are two possible reasons for the formation of the peaks in the thermostated regions: first, the thermal conductivity could be altered by the thermostats (see Sec. II B and Fig. 3 in the Supplemental Material [26]) and, second, the thermal conductivity could be partially ballistic, which would lead to Kapitza-type contacts. The distinction between these two effects is not straightforward and would only be necessary for small amounts of iron on the surfaces where ballistic heat transport is expected. The central results of this work concern CNTs with large amounts of iron atoms on the surfaces. Since these atoms act as scattering centers for phonons, the mean free path between two scattering events is small compared to the length of the CNTs. We therefore assume in the following that thermal conduction is completely diffusive in all our systems. This gives a good approximation for CNTs with large amounts of iron atoms on the surfaces, but we would like to mention that this is only an estimate for the thermal resistances. As the amount of impurity atoms on the surface becomes smaller, the expected deviations from this assumption will become larger. However, as already mentioned, the central statements of this paper are not affected by this detail.

At temperatures that are low compared to the Debye temperature, the neglect of quantum mechanical effects in classical MD also affects the results, usually leading to an overestimation of the thermal conductivity [27,28]. Correction schemes have been proposed to incorporate quantum effects (e.g., [29]), but these are the subject of current research and do not currently provide satisfactory results. An alternative would be modeling using nonequilibrium Green's function approaches, which, however, does not allow the efficient simulation of systems such as the CNTs with foreign atoms on the surfaces discussed in this paper. Overall, the proper treatment of quantum mechanical effects on the thermal conduction of low-dimensional systems such as CNTs and graphene is a complex topic whose treatment is beyond the scope of this paper. The focus of this work is to compare the thermal conduction properties of SWNTs with those of DWNTs discussed in the following sections. Since quantum mechanical corrections can be expected to affect both systems similarly, we do not expect a significant influence on our results.

Under the described assumption, we obtain the temperature gradient along the CNT axis by fitting a linear function to the temperature profiles in the regions not coupled to the thermostats and calculate the thermal resistances using Fourier's law,

$$R_{\mathrm{th}} = \frac{\Delta T}{\dot{Q}}.$$

Figure 3 shows the thermal resistances of bare and iron-covered (10,10) SWNTs with lengths between 17 and 456 nm. The thermal resistance of all CNTs increases significantly with their length and the amount of iron on their surface. Attaching an amount of only 2–5% iron to the surface is sufficient to increase the thermal resistance by one order of magnitude. This effect can be explained by the reduced mean free path of phonons, which can be scattered at the attached iron atoms.

This part of our work has some similarities with a study by Padgett and Brenner [18]. They report 3D thermal

conductivities for (10,10) SWNTs, assuming that the cross-sectional area of a CNT is given by a ring with a thickness of 3.4 Å. Using the same definition with our data, we obtain a 3D conductivity of 479 W/(m K) for bare SWNTs with a length of 456 nm, which are the longest in our calculations. This value roughly agrees with the value of 340 W/(m K) determined by Padgett and Brenner for a 310-nm-long CNT. In our calculations, the specific thermal resistance still decreases with length, while Padgett and Brenner already observe saturation for their longest CNTs. Similar to our work, they observe a drastic decrease in thermal conductivities when they attach phenyl groups to the surfaces.

Mingo and Broido [30] present a theoretical calculation predicting an increase in the thermal conductivities of bare (10,0) SWNTs with $l^{1/3}$ in the lowest-order approximation up to a length of at least 1 μm. This results in a $l^{2/3}$ behavior for the thermal resistances, which agrees well with our results and is illustrated by the dashed line in Fig. 3. To measure thermal conductivities experimentally, CNT lengths of about 2.5 μm are commonly used [6]. Employing the $l^{1/3}$ scaling to extrapolate our data to nanotube lengths of 2.5 μm, we obtain a thermal conductivity of 1064 W/(m K) for bare CNTs. Experimentally measured conductivities are usually in the range of 2000–3500 W/(m K) [6]. Considering that CNT diameters are difficult to measure in experiments and considering possible deficiencies of the chosen empirical potentials [31], our results are in good agreement with the experimental data.

Our results allow for a rough estimate of the thermal conductivities of composites with CNTs. We assume that the CNTs are enclosed in a cubic block of matrix material with temperatures T_1 and T_2 at the ends. Furthermore, we assume that the CNTs are long enough that thermal transport is completely diffusive and that their axes are oriented parallel to each other and parallel to the temperature gradient. Thus, the cross-sectional area of a slice of the material is reduced by the cross section of the CNTs. Due to the different thermal conductivities, the temperature profiles in the matrix and in the CNTs will influence each other. If the number of CNTs in the matrix is rather small, these changes will be limited to the direct surrounding of the CNTs, while the matrix will behave largely like the matrix material without CNTs. For a simple estimate of the thermal conductivity of the composite, we neglect the contact resistance between the matrix and the CNTs and neglect the temperature changes in the surrounding of the CNTs. Under these assumptions, both the CNTs and the matrix will show the same linear temperature profile and a total amount of heat,

$$\begin{aligned}\dot{Q}_{\mathrm{tot}} &= \dot{Q}_{\mathrm{M}} + n\,\dot{Q}_{\mathrm{CNT}} \\ &= \frac{T_2 - T_1}{l}\left[\lambda_{\mathrm{M}}\left(A - n\,\pi\,r_{\mathrm{CNT}}^2\right) + \lambda_{\mathrm{CNT}} n\,2\pi\,r_{\mathrm{CNT}}\right],\end{aligned}$$

is transported through the composite with a total cross-sectional area A with n embedded CNTs. We want to point out that the thermal conductivity of the matrix λ_{M} is a 3D conductivity, while the conductivity of the CNTs λ_{CNT} is a 2D conductivity. With the total thermal conductivity,

$$\lambda_{\mathrm{tot}} = \frac{\dot{Q}_{\mathrm{tot}}\,l}{A\,(T_2 - T_1)},$$

the ratio

$$\frac{\lambda_{\mathrm{tot}}}{\lambda_{\mathrm{M}}} = 1 + \frac{n\,\pi\,r_{\mathrm{CNT}}^2}{A}\left(\frac{\lambda_{\mathrm{CNT}}}{\lambda_{\mathrm{M}}}\,\frac{2}{r_{\mathrm{CNT}}} - 1\right)$$

between the total conductivity and the conductivity of the matrix results. This in turn gives a simple condition for an increase in thermal conductivity with respect to the matrix,

$$1 < \alpha := \frac{\lambda_{\mathrm{CNT}}}{\lambda_{\mathrm{M}}}\,\frac{2}{r_{\mathrm{CNT}}} = \frac{l}{R_{\mathrm{CNT}}\,\lambda_{\mathrm{M}}}\,\frac{1}{\pi\,r_{\mathrm{CNT}}^2}. \tag{1}$$

Using the values from our simulations for the longest CNTs without attached atoms, we obtain $\alpha = 12.3$ for an iron matrix with a thermal conductivity of 80.2 W/(m K). Using the typical heat sink materials aluminum and copper, we obtain values of $\alpha = 4.2$ and $\alpha = 2.5$, respectively. Considering that attaching atoms to the surface can easily increase the thermal resistance of a CNT by one order of magnitude and that the contact resistance between the matrix and the CNT has been neglected, it seems questionable whether adding SWNTs to a metal matrix can have a positive effect on its thermal conductivity. Even if an increase could be observed, it can be assumed that the influence will be rather small. On the other hand, the values of α obtained under the described assumptions allow for speculation about a much higher influence of MWNTs on the thermal conductivity of the composite since their inner walls will also contribute. In the following sections, the influence of double-walled CNTs on composites will be investigated in detail.

B. (10,10)-(15,15) DWNTs

As long as there are no chemical bonds between the concentric walls of MWNTs, the individual walls interact only via weak van der Waals forces. Therefore, one can speculate that the inner walls, which are not in direct contact with the matrix, might be protected against it by the outer layers and retain their high thermal conductivities. To test this hypothesis, we simulate (10,10)-(15,15) DWNTs in which the thermostats are coupled to the (10,10) walls [Fig. 1(c)] and iron atoms are attached only to the (15,15) walls. This choice allows a direct comparison of the thermal conductivities with those of the (10,10) SWNTs described in Sec. III A.

The temperature profiles in the two walls of a DWNT differ from those in a SWNT due to interwall coupling (Fig. 4). Similar to the SWNTs, we solve the heat equation for this system to obtain a model for the temperature profiles and fit it to the temperature profiles recorded in our simulations. The solution is only briefly described here; a detailed discussion can be found in Sec. III of the Supplemental Material [26].

The total amount of heat per time $\dot{Q}_{\mathrm{i}}$ flowing into or out of the inner wall of a DWNT is obtained by integrating the heat current over a cylindrical closed surface V_{i} enclosing the inner wall,

$$\dot{Q}_{\mathrm{i}} = -\oint_{V_{\mathrm{i}}} \mathbf{j}_{\mathrm{i}} \cdot d\mathbf{S} - \oint_{V_{\mathrm{i}}} \mathbf{j}_{\mathrm{io}} \cdot d\mathbf{S},$$

with a heat current $\mathbf{j}_{\mathrm{i}}$ through the ends of the CNT and a current $\mathbf{j}_{\mathrm{io}}$ between the inner and the outer wall. Using Fourier's law for $\mathbf{j}_{\mathrm{i}}$, applying Gauss's theorem for the first integral, and

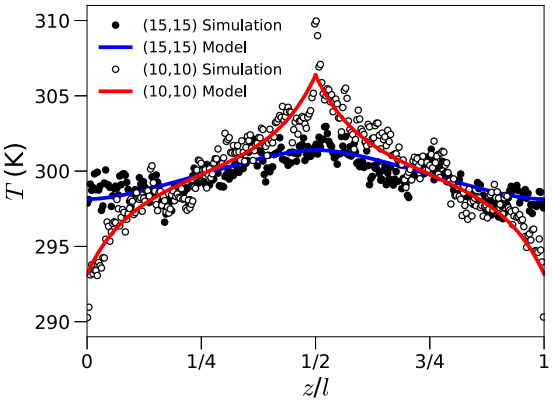

FIG. 4. Temperature profiles in the two walls of a 114-nm-long (10,10)-(15,15) DWNT with 2% iron atoms attached to the surface of the outer wall. The red and blue lines show a χ^2 fit of a theoretical model to the data (see text for details).

using the expression

$$\mathbf{j}_{\mathrm{io}}(\mathbf{r})\Big|_{||\mathbf{r}||=r_{\mathrm{i}}} = -\kappa_{\mathrm{io}}\frac{T_{\mathrm{o}}(x)-T_{\mathrm{i}}(x)}{r_{\mathrm{o}}-r_{\mathrm{i}}}\,\hat{\mathbf{n}}_r$$

for the heat flux between the inner and the outer wall with the coupling constant κ_{io} leads to

$$\dot{Q}_{\mathrm{i}} = \lambda_{\mathrm{i}}\,2\pi\,r_{\mathrm{i}}\int_{x_1}^{x_2}\frac{d^2}{dx^2}T_{\mathrm{i}}(x)\,dx + \kappa_{\mathrm{io}}\,2\pi\,r_{\mathrm{i}}\int_{x_1}^{x_2}\frac{T_{\mathrm{o}}(x)-T_{\mathrm{i}}(x)}{r_{\mathrm{o}}-r_{\mathrm{i}}}\,dx.$$

With a similar calculation for the outer wall and the condition of vanishing change of heat density at the surface in equilibrium, we obtain the system of differential equations

$$0 = \lambda_{\mathrm{i}}\frac{d^2}{dx^2}T_{\mathrm{i}}(x) + \kappa_{\mathrm{io}}\frac{1}{r_{\mathrm{o}}-r_{\mathrm{i}}}\big[T_{\mathrm{o}}(x)-T_{\mathrm{i}}(x)\big],$$

$$0 = \lambda_{\mathrm{o}}\frac{d^2}{dx^2}T_{\mathrm{o}}(x) - \kappa_{\mathrm{io}}\frac{r_{\mathrm{i}}}{r_{\mathrm{o}}}\frac{1}{r_{\mathrm{o}}-r_{\mathrm{i}}}\big[T_{\mathrm{o}}(x)-T_{\mathrm{i}}(x)\big],$$

with the solution

$$T_{\mathrm{i}}(x) = A_1 e^{\omega x} + A_2 e^{-\omega x} + A_3\,x + A_4,$$

$$T_{\mathrm{o}}(x) = B_1 e^{\omega x} + B_2 e^{-\omega x} + B_3\,x + B_4.$$

By fitting this model to the recorded temperature profiles (Fig. 4), we obtain the thermal resistances of the DWNTs. Figure 5(a) shows the results of these calculations compared to the thermal resistances of (10,10) SWNTs. It can be clearly seen that the specific thermal resistances of DWNTs are almost unaffected by attaching iron atoms to the surfaces of the outer walls, while the specific resistances of (10,10) SWNTs increase drastically. From these results, we conclude that the inner walls are indeed protected against the matrix by the outer walls and behave almost like SWNTs in vacuum.

C. (5,5)-(10,10) DWNTs

Besides protecting the inner walls against the matrix, one could imagine that additional walls on the inside could support the thermal conduction of the outer walls. Heat could be transferred from the outer to the inner wall and phonons could propagate through the inner wall, which has a considerably lower thermal resistance than an outer wall covered with foreign atoms. In this way, the increase in thermal resistance could be less pronounced than for SWNTs. To test this hypothesis, we calculate the thermal resistances of (5,5)-(10,10) DWNTs and compare them with (10,10) SWNTs. Similar to the calculations in Sec. III B, the thermostats are coupled to the (10,10) walls [Fig. 1(d)] and the thermal resistances are calculated by fitting an analytical model to the temperature profiles. The derivation of the theoretical temperature profiles for these systems is the same as for the (10,10)-(15,15) DWNTs with modified boundary conditions. Details can be found in the Supplemental Material [26].

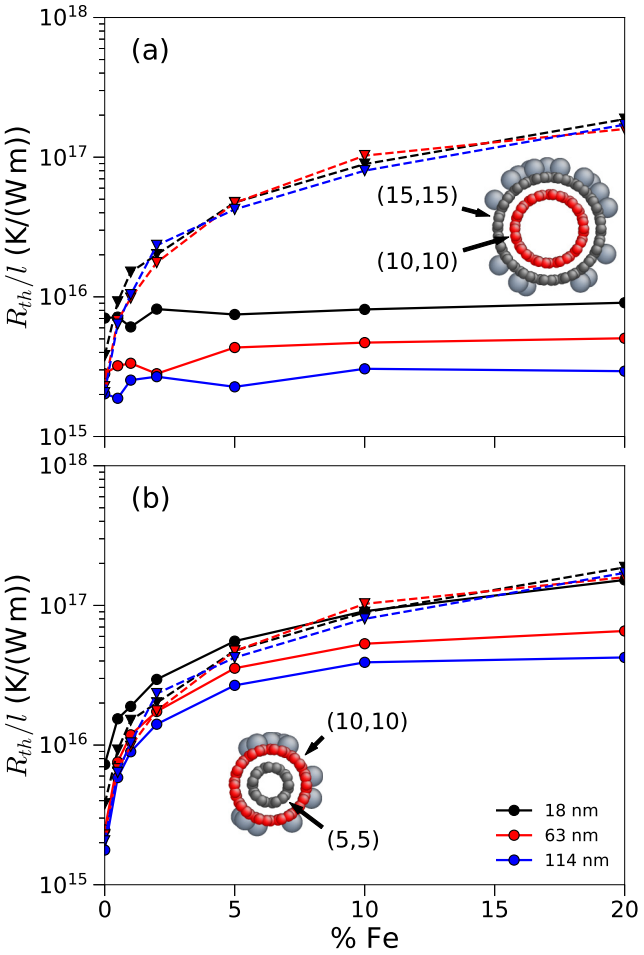

FIG. 5. Specific thermal resistances of (10,10)-(15,15) and (5,5)-(10,10) DWNTs [solid lines in (a) and (b)] compared to the corresponding values for (10,10) SWNTs (dashed lines) with the same amounts of iron on the surfaces. The pictures show sections through the simulated DWNTs, with the walls to which the thermostats are applied marked in red.

Figure 5(b) shows the results of these calculations. It can be clearly seen that an additional wall on the inside has almost no influence on the thermal resistance of 18-nm-long DWNTs. As the length increases, the influence of the inner wall increases and the thermal resistances of iron-covered DWNTs

are reduced compared to SWNTs. The specific resistance of a 114-nm-long (5,5)-(10,10) DWNT with 20% Fe on the surface, for example, is lower by a factor of 5 than that of a (10,10) SWNT. These results are consistent with the assumption that heat is transferred to inner walls and back since the distance that phonons can travel on the inner wall without being scattered increases with CNT length. Nevertheless, the thermal resistances of (5,5)-(10,10) DWNTs increase with the amount of iron on the surface, and even for the longest CNTs, the thermal resistance is still more than an order of magnitude higher than that of a (10,10)-(15,15) DWNT in which the thermostats are directly coupled to the inner wall. In theory, a supporting effect and a slight decrease in thermal resistance should also be visible for (10,10)-(15,15) DWNTs compared to (10,10) SWNTs due to heat transfer to the other wall, but one can expect this effect to be very weak and we did not observe it in our simulations.

D. Composites with DWNTs

Using the same assumptions and estimations presented in Sec. III A, we obtain the condition

$$1 < \alpha := \frac{l}{R_{\mathrm{CNT}}\,\lambda_{\mathrm{M}}}\,\frac{1}{\pi r_{\mathrm{CNT,o}}^2},$$

for the increase in thermal conductivity of a DWNT-containing composite, where $r_{\mathrm{CNT,o}}$ is the radius of the outer CNT wall. In the previous section, we showed that the thermal resistance of a DWNT with large amounts of iron atoms on the surface of the outer wall can be easily reduced by a factor of 5 from an additional inner wall, even if the only thermal coupling of the inner wall to the heat source is the weak van der Waals interaction between the different walls [Fig. 5(b)]. We have also shown that the inner wall of a DWNT behaves almost like a SWNT in vacuum and that its thermal resistance is independent of the amount of foreign atoms coupled to the outer wall [Fig. 5(a)]. Direct thermal contact between the inner wall and the matrix, i.e., open CNT ends, should therefore have a drastic effect on the composite conductivity. Considering the estimated values for α from Sec. III A, it should be much easier to reach the regime of increased thermal conductivity if DWNTs are used. This result is in good agreement with the work of Moisala *et al.* [19], who observed an increase for MWNTs in a polymer composite and a decrease for SWNTs.

In general, it should be beneficial to use MWNTs with a large number of walls. This is especially interesting for technical applications since production of MWNTs is easier and cheaper than the production of SWNTs. Removal of the end caps should be sufficient to achieve direct thermal coupling between the inner walls and the matrix. This has been shown to be a fairly simple task and can be achieved by simply heating the CNTs in air [32] or in carbon dioxide [33].

We expect that the described shielding of the inner walls against the matrix should also be relevant for composites containing multilayer graphene. Since multilayer graphene is easy to produce, e.g., by ball milling of graphite [34], experimental validations and eventual technical applications should be easy to realize.

IV. CONCLUSIONS

We have shown that there are significant differences between the thermal transport in SWNTs and DWNTs when the outer walls are in contact with foreign atoms. While the thermal resistance of a SWNT increases drastically when foreign atoms are attached to its surface, the inner wall of a DWNT is not affected by foreign atoms on the outer wall and behaves almost like a SWNT in vacuum. Therefore, the use of MWNTs with a large number of walls should be advantageous for the production of composites with enhanced thermal conductivity. There should be no covalent bonds between the walls, and the end caps of the CNTs should be removed to allow for direct coupling between the composite matrix and the inner walls.

ACKNOWLEDGMENTS

Parts of this work have been funded by the German Bundesministerium für Bildung und Forschung BMBF (Project CarboMetal) and the Deutsche Forschungsgemeinschaft DFG (Grant No. MO 879/21-1). Atomistic simulations have been carried out at the Jülich Supercomputing Centre (Grant No. hfr09).

[1] R. M. Sundaram, A. Sekiguchi, M. Sekiya, T. Yamada, and K. Hata, R. Soc. Open Sci. **5**, 180814 (2018).

[2] J. Stein, B. Lenczowski, N. Frety, and E. Anglaret, Carbon **50**, 2264 (2012).

[3] C. Karch, B. Lenczowski, Y. Yeshurun, and J. Wolfrum, Structural component: Hybrid lightning protection of CFRP/GFRP structures with CNT non-woven mats, European Patent Appl. No. EP 16 164 424.0 (2016), U.S. Patent Appl. No. 15/471795 (2017).

[4] A. Miranda, N. Barekar, and B. J. McKay, J. Alloys Compd. **774**, 820 (2019).

[5] H. Zhan, Y. Nie, Y. Chen, J. M. Bell, and Y. Gu, Adv. Funct. Mater. **30**, 1903841 (2020).

[6] J. R. Lukes and H. Zhong, J. Heat Transfer **129**, 705 (2007).

[7] D. R. Lide, *CRC Handbook of Chemistry and Physics* (CRC Press, Boca Raton, FL, 2008).

[8] K. Kordas, G. Toth, P. Moilanen, M. Kumpumäki, J. Vähäkangas, A. Uusimäki, R. Vajtai, and P. M. Ajayan, Appl. Phys. Lett. **90**, 123105 (2007).

[9] L. Ping, P. Hou, C. Liu, and H. Cheng, APL Mater. **7**, 020902 (2019).

[10] A. Yu, M. E. Itkis, E. Bekyarova, and R. C. Haddon, Appl. Phys. Lett. **89**, 133102 (2006).

[11] M. J. Biercuk, M. C. Llaguno, M. Radosavljevic, J. K. Hyun, A. T. Johnson, and J. E. Fischer, Appl. Phys. Lett. **80**, 2767 (2002).

[12] E. S. Choi, J. S. Brooks, D. L. Eaton, M. S. Al-Haik, M. Y. Hussaini, H. Garmestani, D. Li, and K. Dahmen, J. Appl. Phys. **94**, 6034 (2003).

[13] M. B. Jakubinek, M. A. White, M. Mu, and K. I. Winey, Appl. Phys. Lett. **96**, 083105 (2010).
[14] M. Liu, H. Younes, H. Hong, and G. P. Peterson, Polymer **166**, 81 (2019).
[15] C. Kim, B. Lim, B. Kim, U. Shim, S. Oh, B. Sung, J. Choi, J. Ki, and S. Baik, Synth. Met. **159**, 424 (2009).
[16] K. Chu, Q. Wu, C. Jia, X. Liang, J. Nie, W. Tian, G. Gai, and H. Guo, Compos. Sci. Technol. **70**, 298 (2010).
[17] S. T. Huxtable, D. G. Cahill, S. Shenogin, L. Xue, R. Ozisik, P. Barone, M. Usrey, M. S. Strano, G. Siddons, M. Shim, and P. Keblinski, Nat. Mater. **2**, 731 (2003).
[18] C. W. Padgett and D. W. Brenner, Nano Lett. **4**, 1051 (2004).
[19] A. Moisala, Q. Li, I. A. Kinloch, and A. H. Windle, Compos. Sci. Technol. **66**, 1285 (2006).
[20] S. H. Boroushak, R. Ansari, and S. Ajori, Diam. Relat. Mater. **86**, 173 (2018).
[21] J. Tersoff, Phys. Rev. B **39**, 5566 (1989).
[22] D. W. Brenner, Phys. Rev. B **42**, 9458 (1990).
[23] K. O. E. Henriksson and K. Nordlund, Phys. Rev. B **79**, 144107 (2009).
[24] L. A. Girifalco, M. Hodak, and R. S. Lee, Phys. Rev. B **62**, 13104 (2000).
[25] Z. Xia and W. A. Curtin, Phys. Rev. B **69**, 233408 (2004).
[26] See Supplemental Material at http://link.aps.org/supplemental/10.1103/PhysRevMaterials.5.086001 for a detailed derivation of temperature profiles in single- and double-walled CNTs.
[27] E. Pop, V. Varshney, and A. K. Roy, MRS Bull. **37**, 1273 (2012).
[28] Z. Xu, Theor. Appl. Mech. Lett. **6**, 113 (2016).
[29] J. Hu, X. Ruan, and Y. P. Chen, Nano Lett. **9**, 2730 (2009).
[30] N. Mingo and D. A. Broido, Nano Lett. **5**, 1221 (2005).
[31] L. Lindsay and D. A. Broido, Phys. Rev. B **81**, 205441 (2010).
[32] P. M. Ajayan, T. W. Ebbesen, T. Ichihashi, S. Iijima, K. Tanigaki, and H. Hiura, Nature (London) **362**, 522 (1993).
[33] S. C. Tsang, P. J. F. Harris, and M. L. H. Green, Nature (London) **362**, 520 (1993).
[34] I. Y. Jeon, Y. R. Shin, G. J. Sohn, H. J. Choi, S. Y. Bae, J. Mahmood, S. M. Jung, J. M. Seo, M. J. Kim, W. C. D., L. Dai, and J. B. Baek, Proc. Natl. Acad. Sci. **109**, 5588 (2012).